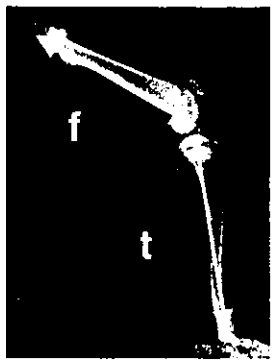

Femoral length (arrow f) and tibial length (arrow t) were measured radiographically.

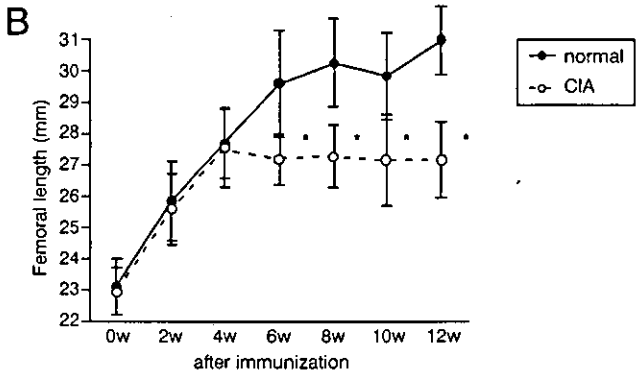

No growth of femur was observed in CIA rats after week 4 (solid line, normal; dotted line, CIA).

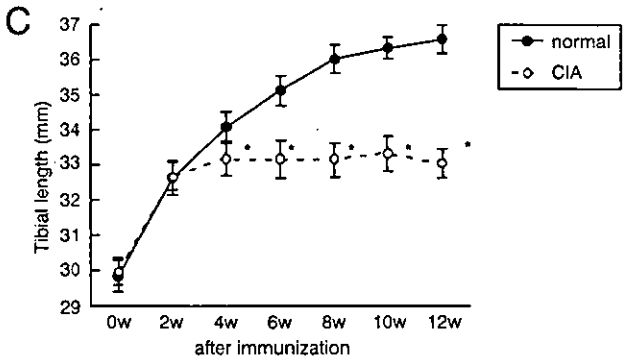

No growth of tibia was observed in CIA rats after week 2 (solid line, normal; dotted line, CIA).
(Values shown are mean ±SD. *=p<0.01, versus normal rats.)

Figure 2. Length of femur and tibia at times following immunization.

E1000; Nikon, Tokyo, Japan) at 200x magnification, and the microscopic images were displayed on a computer. The widths of the whole growth plate, proliferating zone, and hypertrophic zone of the proximal tibial growth plate were measured at 3 sites for each section using Photoshop (Adobe Systems Incorporated, CA, USA). The mean widths were then calculated (Figure 7A).

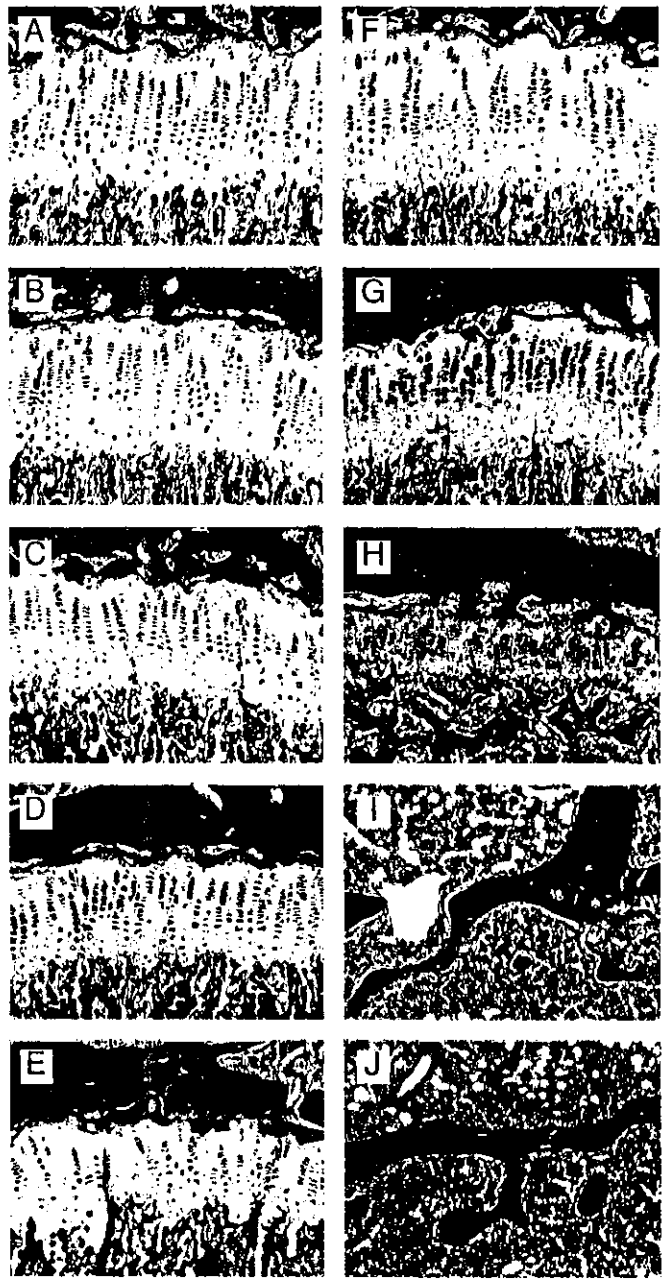

Figure 3. Growth plate proximal tibia (hematoxylin and eosin, 200x).
(A-E) Normal rats. The epiphyseal growth plate of the proximal tibia was composed of very regular columns in the 8-week-old normal rats. The width of growth plate decreased slowly, but the regular arrangement and properties of cells in the column were well conserved until 18 weeks of age (A, 8 weeks old; B, 9 weeks old; C, 10 weeks old; D, 12 weeks old; E, 18 weeks old).
(F-J) CIA rats. Nearly normal column formation in growth plate was observed in the CIA rats at 2 weeks after immunization (age, 8 weeks) (F). The proliferating zone cells appeared swollen at 3 weeks after immunization (G). The width of the hypertrophic cell zone was greatly reduced at 4 weeks after immunization (H). The width of the hypertrophic cell zone was then reduced until it finally disappeared at 12 weeks after immunization (age, 18 weeks) (J). (F, 8 weeks old; G, 9 weeks old; H, 10 weeks old; I, 12 weeks old; J, 18 weeks old).

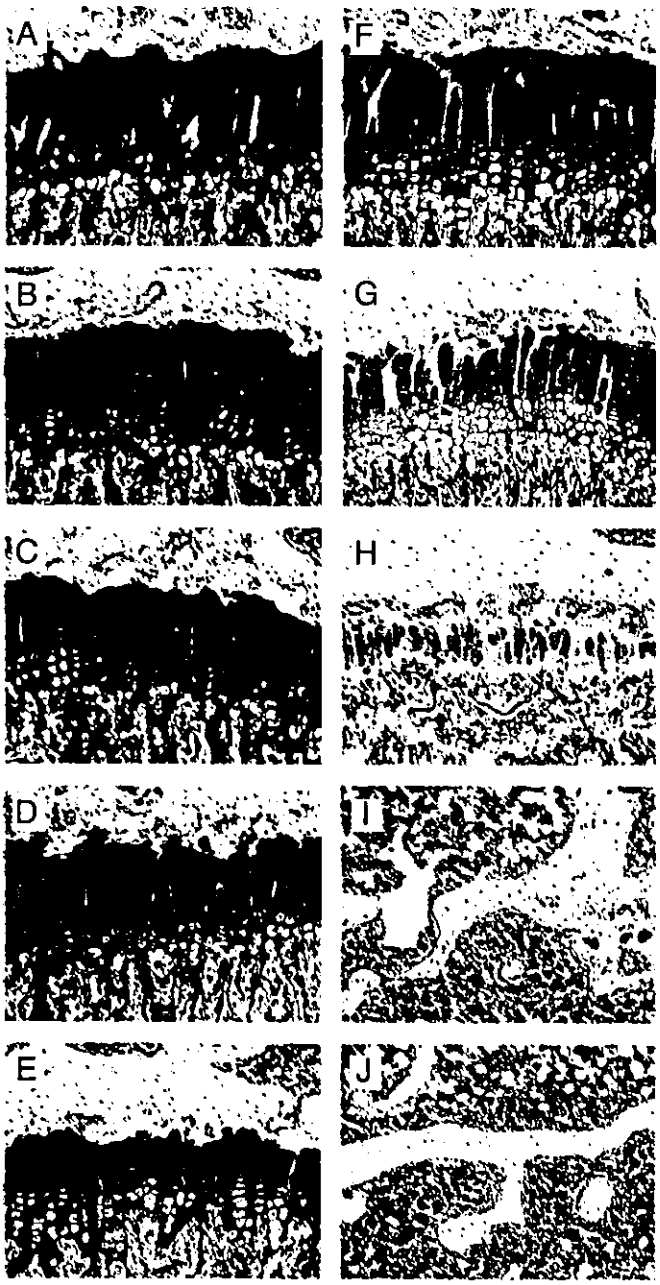

Figure 4. Growth plate of proximal tibia (safranin-O staining, 200x). (A-E) Normal rats. (A, 8 weeks old; B, 9 weeks old; C, 10 weeks old; D, 12 weeks old; E, 18 weeks old).
(F-J) CIA rats. (F, 8 weeks old; G, 9 weeks old; H, 10 weeks old; I, 12 weeks old; J, 18 weeks old).
Intensity of safranin-O staining was well conserved from 8 to 18 weeks of age in the normal rats (A-E), whereas it was decreased at 8 and 9 weeks of age in CIA rats (2 and 3 weeks after immunization, respectively).

Statistical analysis

All data were expressed as the mean ± SD, and statistical analysis was performed with the Mann-Whitney U test. Differences were considered significant if p value was less than 0.01.

Results

Epiphyseal growth plate closure in CIA rats

In normal (control) rats, the growth plate widths gradually decreased with age, from 6 to 18 weeks (Figure 1A-C). The growth plate widths decreased more rapidly with age in the CIA rats and were essentially closed by 18 weeks (Figure 1D and E).

Length of femur and tibia

Femoral lengths of the normal and CIA groups increased in a similar manner until 4 weeks after immunization. After six weeks substantial differences were observed between the normal and CIA groups. In the normal group, femoral length continued to increase throughout the experiment, but the femoral length of the CIA group was nearly constant from 4 to 12 weeks after immunization (Figure 2B).

In CIA rats, the growth curve of the tibia was similar to that of the femur. In normal rats, tibial length increased throughout the experiment, while in the CIA rats there was little increase from 2 to 12 weeks after immunization (Figure 2C). There were significant differences in femoral length after 6 weeks and tibial length after 4 weeks between normal rats and CIA rats (Figure 2B and C).

Histology of the growth plate

The epiphyseal growth plate of the proximal tibia was composed of very regular columns[12]. In normal rats, the width of the growth plate decreased with age, but the regular arrangement and properties of cells in the columns remained well conserved through the experimental period (18 weeks of age) (Figure 3A-E).

In the CIA rats, the growth plates appeared essentially normal for the first 2 weeks after immunization (age, 8 weeks) (Figure 3F). Beginning at 3 weeks, there were striking alterations in the morphology of the epiphyseal growth plate of the CIA rats (Figure 3G). The proliferating cells appeared enlarged, and columns of chondrocytes had become irregular. The width of the hypertrophic zone was significantly less in CIA rats compared with the normal rats. In the CIA rats, the hypertrophic zone was no longer evident by 4 weeks after immunization (Figure 3H), and the epiphyseal growth plate was almost gone by 6 weeks after immunization and was essentially absent by 12 weeks after immunization (Figure 3 I and J).

There were also differences in safranin-O staining of the growth plate between normal and CIA rats. In normal rats, intensity of safranin-O staining remained at the same level from 6 to 18 weeks of age (Figure 4A-E), whereas, in CIA rats, the intensity decreased beginning 2 weeks after immunization (age, 8 weeks) (Figure 4F-J).

Immunohistochemical evaluation of growth plate

Immunohistochemical detection and localization of MMP-3 and VEGF showed that these proteins were expressed in hypertrophic chondrocytes in the growth plates from 8-week-old normal and CIA rats at 2 weeks after immunization (Figure 5A, 5C, 6A and 6C). By 3 weeks after immunization (age, 9 weeks), significant differences were seen between normal and CIA rats. In normal rats, these proteins were detected only in hypertrophic chondrocytes (Figure 5B and 6B), while the enlarged chondrocytes in the proliferating zone from CIA rats also expressed these proteins. The relative number of chondrocytes expressing these proteins increased in the CIA rats (Figure 5D and 6D).

Widths of whole growth plate and proliferating and hypertrophic zones

In the normal rats, the widths of the whole growth plate and hypertrophic zone decreased with age, but growth plate was still evident at 18 weeks of age (same age as CIA rats at 12 weeks after immunization). In the CIA rats, there were rapid decreases in growth plate width with age, especially in the hypertrophic zone. The widths of the proliferating zone also decreased with age, but less rapidly than the hypertrophic zone. At 6 weeks after immunization (age, 12 weeks), growth plate had essentially disappeared (Figures 7B-D).

Discussion

Although CIA is a widely used experimental model of rheumatoid arthritis[13-16], few studies have focused on the pathological changes in the epiphyseal growth plate[4]. In this study, we demonstrated that growth disturbances of long bones occurred during the development of arthritis in the CIA rat model. The longitudinal growth retardation was recognised radiographically in the tibia and femur from 4 weeks after immunization, and the pathological epiphyseal closure was recognised radiographically and histologically at 6 weeks after immunization. Finally, at 12 weeks after immunization, tibial and femoral average lengths in the CIA rats were 3.8mm (12.2% of normal length) and 3.6 mm (9.7% of normal length), respectively, shorter than those in the control rats. These results indicated that pathological epiphyseal closure occurs in CIA rats, and resulted in longitudinal growth retardation of the tibia and femur.

A decrease in safranin-O staining of the growth plates in the CIA rats was evident prior to morphological changes in the chondrocytes. There was a later diminution of the growth plate width, particularly evident in the hypertrophic zone. Since the intensity of safranin-O staining correlates with the amounts of proteoglycans in cartilage[17], the reduced staining of the growth plates in the CIA rats suggests a decreased production and/or an increased degradation of proteoglycans. MMP-3 is a stromelysin, which degrades proteoglycans[18,19]. In this study we showed an increase of MMP-3 producing cells in the growth plates of CIA rats. These findings suggest that over expressed MMP-3 could result in increased proteoglycan degradation in the growth plates of CIA rats.

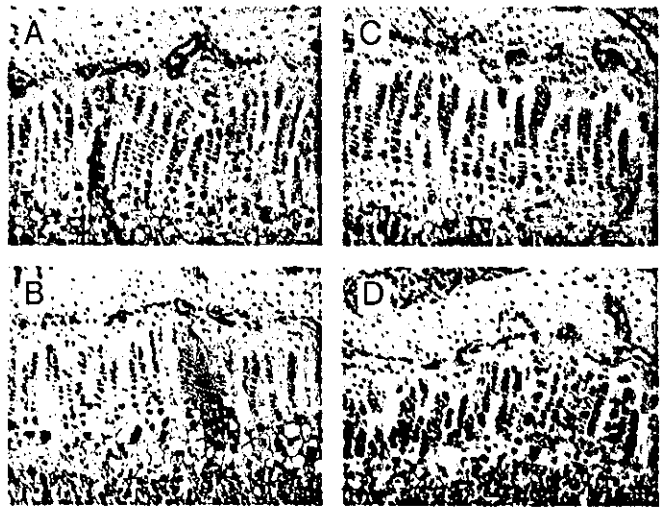

Figure 5. Growth plate of proximal tibia (immunohistochemistry against MMP-3, 200x).
(A, B) Normal rats. (A, 8 weeks old; B, 9 weeks old).
(C, D) CIA rats. (C, 8 weeks old; D, 9 weeks old).
Immunohistochemistry against MMP-3 shown the immunoreactivity was seen in hypertrophic chondrocytes in growth plate of 8 week-old rats (A and C). MMP-3 positive cells were increasing in CIA rats of 9 weeks of age (3 weeks after immunization) than that of normal rats (B and D, respectively).

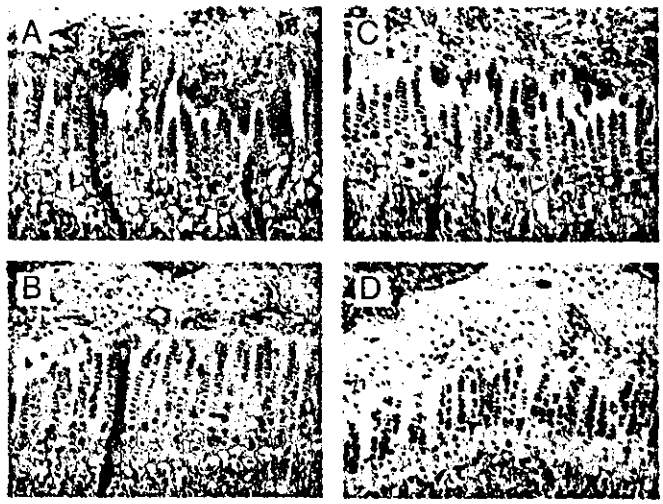

Figure 6. Growth plate of proximal tibia (immunohistochemistry against VEGF, 200x).
(A, B) Normal rats. (A, 8 weeks old; B, 9 weeks old).
(C, D) CIA rats. (C, 8 weeks old; D, 9 weeks old).
Immunohistochemistry against VEGF shown the immunoreactivity were seen in hypertrophic chondrocytes in growth plate of 8-week-old rats (A and C). Increase of VEGF-positive cells were seen in CIA rats of 9 weeks of age (3 weeks after immunization) than that of rats (B and D, respectively). Immunoreactivity against VEGF was also detected in swollen shaped chondrocytes in proliferating zone of CIA rats at 9 weeks of age.

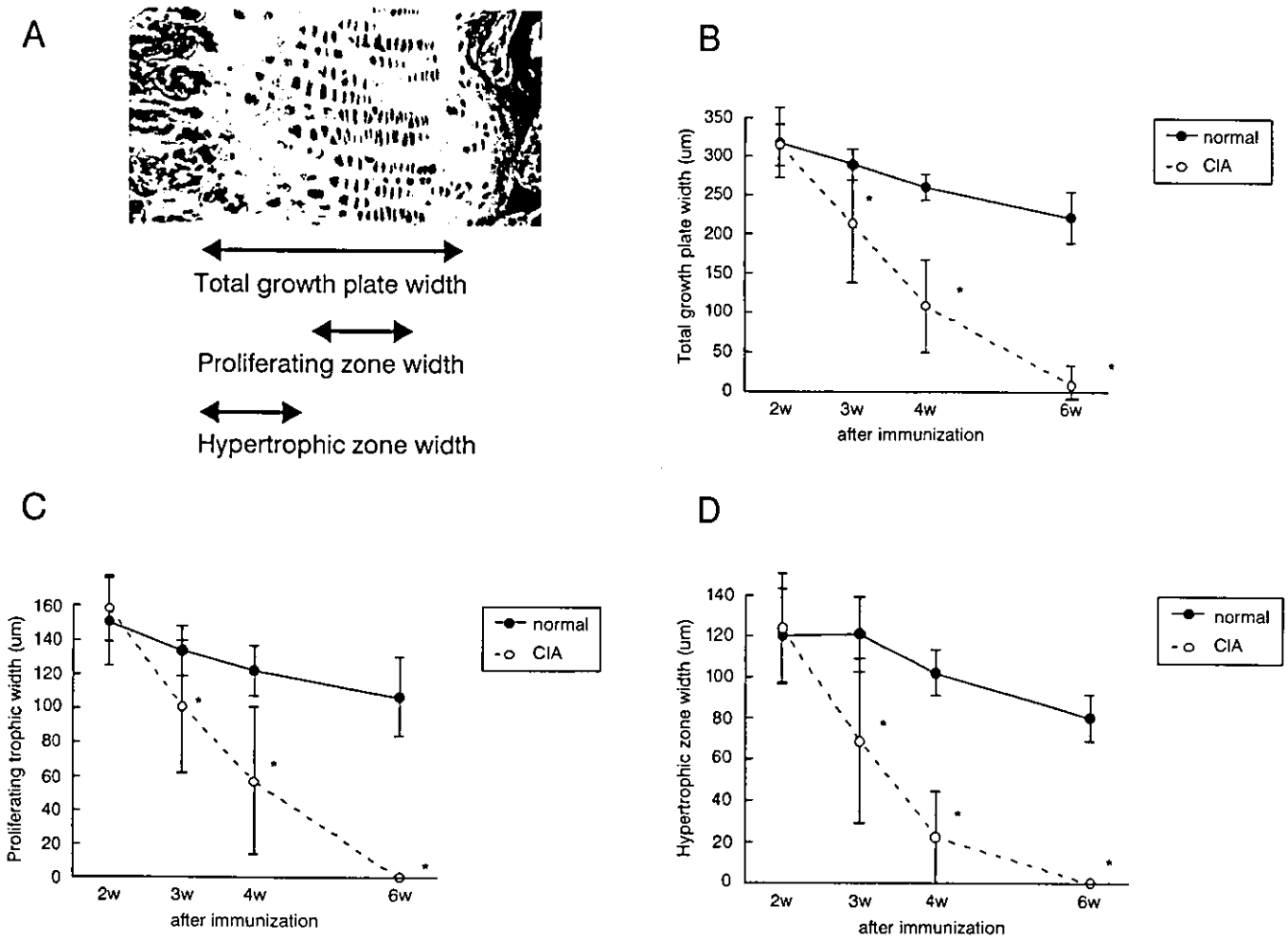

Figure 7. Growth plate widths at times following immunization.
(A) Total width, proliferating zone width, and hypertrophic zone width of growth plate in proximal tibia were measured.
(B) Total width of growth plate decreased more rapidly in CIA rats than in normal rats, and was greatly diminished 6 weeks after immunization (solid line, normal; dotted line, CIA).
(C, D) The decrease of hypertrophic zone width was more prominent than the decrease of proliferating zone width in CIA rats 3 and 4 weeks after immunization.

In this animal model of arthritis, it was clearly shown that such proinflammatory cytokines like TNF-α and IL-1β are involved in the pathogenesis of the disease, although there are a few reports concerning cytokine levels in the bone marrow in animals with CIA[20]. TNF-α and IL-1β are also implicated in the induction of MMPs, such as MMP-1 and MMP-3. These MMPs are involved in the degradation of the ECM[18,19,21-23]. The increase of MMP-3 producing cells in the growth plate of CIA might be the consequence of the greater production of proinflammatory cytokines in the bone marrow.

In addition, proteoglycan synthesis by chondrocytes could be affected by proinflammatory cytokines, which may lead to a decrease of proteoglycans in cartilage and decreased intensity of safranin-O staining.

During normal growth of the epiphyseal plate, stem cells initiate their programmed differentiation by frequent proliferation and typical columnar arrangement. Subsequently, cells cease proliferating and change morphometrically into their hypertrophic shape.

These hypertrophic chondrocytes mature further to produce matrix components. Thereafter matrix around the hypertrophic chondrocytes calcifies and the chondrocytes undergo apoptosis. These calcified matrices are replaced with trabecular bone by osteoclasts/chondroclasts and osteoblasts[12,25,26].

Various families of molecules have been identified as participating in the growth and development of bone[26-35]. Among these molecules, VEGF has been shown to be a key regulator of neoangiogenesis in cartilage growth plate, apoptosis of hypertrophic chondrocytes and osteoclasts recruitment into hypertrophic cartilage[36-38]. The present study demonstrates that the destruction of the growth plate in CIA

rats was accompanied with morphological changes of the hypertrophic chondrocytes and with an increase in the number of VEGF expressing cells. These findings suggest that over expressed VEGF in the growth plates of CIA rats might be involved with the abnormal ossification of the matrix and perhaps an increased recruitment of osteoclasts/chondroclasts, which resulted in destruction of the growth plate cartilage.

Many papers have assessed antiarthritic effectiveness of various molecules using the CIA model, however, the changes in growth plate cartilage have not been carefully evaluated. The quantitative analysis reported by Jee et al. showed a protective effect of methylpredonizolone against growth plate erosion in adjuvant-induced arthritis in rats[4]. This steroid is a well-known and potent anti-inflammatory agent that suppresses the production of inflammatory cytokines and MMPs[39,40]. These reports suggested that the protective effect of the steroid against growth plate erosion could be via suppression of some cytokines and MMPs, supporting some of the observations made in the present study. The detail of this process is still unclear and further investigation is necessary to elucidate the pathogenesis of growth plate destruction in inflammatory conditions. Clarification of the mechanism of this phenomenon could yield clinical benefits, especially in prevention of the premature closure of growth plate that is seen in juvenile rheumatoid arthritis and other diseases. This CIA rat model appears to be a useful model for further studies.

Acknowledgments

The authors thank Fumi Tamaki, Kanae Asai, Kaori Izumi and Shoko Kuroda for their technical expertise. This research was supported by a grant from the Organization for Pharmaceutical Safety and Research and by a Grant-in-Aid for Scientific Research from the Ministry of Education, Science and Culture, Japan.

References

1. Wooley PH. Animal models of rheumatoid arthritis. Curr Opin Rheumatol 1991; 3:407-420.
2. Williams RO, Feldmann M, Maini RN. Anti-tumor necrosis factor ameliorates joint disease in murine collagen-induced arthritis. Proc Natl Acad Sci USA 1992; 89:9784-9788.
3. Badger AM, Blake S, Kapadia R, Sarkar S, Levin J, Swift BA, Hoffman SJ, Stroup GB, Miller WH, Gowen M, Lark MW. Disease-modifying activity of SB 273005, an orally active, non-peptide alphavbeta3 (vitronectin receptor) antagonist, in rat adjuvant-induced arthritis. Arthritis Rheum 2001; 44:128-137.
4. Jee WSS, Li XJ, Ke HZ, Li M, Smith RJ, Dunn CJ. Application of computer-based histomorphometry to the quantitative analysis of methylprednisolone-treated adjuvant arthritis in rats. Bone Miner 1993; 22:221-247.
5. Bunger C, Bunger EH, Harving S, Djurhuus JC, Jensen OM. Growth disturbances in experimental juvenile arthritis of the dog knee. Clin Rheumatol 1984; 3:181-188.
6. Simon S, Whiffen J, Shapiro F. Leg-length discrepancies in monoarticular and pauciarticular juvenile rheumatoid arthritis. J Bone Joint Surg Am 1981; 63:209-215.
7. Trentham DE, Townes AS, Kang AH. Autoimmunity to type II collagen an experimental model of arthritis. J Exp Med 1977; 146:857-868.
8. Damron TA, Spadaro JA, Margulies B, Damron LA. Dose response of amifostine in protection of growth plate function from irradiation effects. Int J Cancer 2000; 90:73-79.
9. Sanchez CP, Salusky IB, Kuizon BD, Abdella P, Juppner H, Goodman WG. Growth of long bones in renal failure: roles of hyperparathyroidism, growth hormone and calcitriol. Kidney Int 1998; 54:1879-1887.
10. Sanchez CP, Kuizon BD, Abdella PA, Juppner H, Salusky IB, Goodman WG. Impaired growth, delayed ossification, and reduced osteoclastic activity in the growth plate of calcium-supplemented rats with renal failure. Endocrinology 2000; 141:1536-1544.
11. Edmondson SR, Baker NL, Oh J, Kovacs G, Werther GA, Mehls O. Growth hormone receptor abundance in tibial growth plates of uremic rats: GH/IGF-I treatment. Kidney Int 2000; 58:62-70.
12. Hunziker EB. Mechanism of longitudinal bone growth and its regulation by growth plate chondrocytes. Microsc Res Tech 1994; 28:505-519.
13. Wooley PH, Luthra HS, Krco CJ, Stuart JM, David CS. Type II collagen-induced arthritis in mice. II. Passive transfer and suppression by intravenous injection of anti-type II collagen antibody or free native type II collagen. Arthritis Rheum 1984; 27:1010-1017.
14. Durie FH, Fava RA, Noelle RJ. Collagen-induced arthritis as a model of rheumatoid arthritis. Clin Immunol Immunopathol 1994; 73:11-18.
15. Myers LK, Rosloniec EF, Cremer MA, Kang AH. Collagen-induced arthritis, an animal model of autoimmunity. Life Sci 1997; 61:1861-1878.
16. Anthony DD, Haqqi TM. Collagen-induced arthritis in mice: an animal model to study the pathogenesis of rheumatoid arthritis. Clin Exp Rheumatol 1999; 17:240-244.
17. Kiraly K, Hyttinen MM, Parkkinen JJ, Arokoski JA, Lapvetelainen T, Torronen K, Kiviranta I, Helminen HJ. Articular cartilage collagen birefringence is altered concurrent with changes in proteoglycan synthesis during dynamic *in vitro* loading. Anat Rec 1998; 251:28-36.
18. Dean DD, Martel-Pelletier J, Pelletier JP, Howell DS, Woessner JF. Evidence for metalloproteinase and metalloproteinase inhibitor imbalance in human osteoarthritic cartilage. J Clin Invest 1989; 84:678-685.
19. Woessner JF. Matrix metalloproteinases and their inhibitors in connective tissue remodeling. FASEB J 1991; 5:2145-2154.

20. Hayashida K, Ochi T, Fujimoto M, Owaki H, Shimaoka Y, Ono K, Matsumoto K. Bone marrow changes in adjuvant-induced and collagen-induced arthritis. Interleukin-1 and interleukin-6 activity and abnormal myelopoiesis. Arthritis Rheum 1992; 35:241-245.
21. Lefebvre V, Peeters-Joris C, Vaes G. Modulation by interleukin-1 and tumor necrosis factor alpha of production of collagenase, tissue inhibitor of metalloproteinases and collagen types in differentiated and dedifferentiated articular chondrocytes. Biochim Biophys Acta 1990; 1052:366-378.
22. Feldmann M, Brennan FM, Maini RN. Role of cytokines in rheumatoid arthritis. Ann Rev Immunol 1996; 14:397-440.
23. Hui A, Min WX, Tang J, Cruz TF. Inhibition of activator protein 1 activity by paclitaxel suppresses interleukin-1-induced collagenase and stromelysin expression by bovine chondrocytes. Arthritis Rheum 1998; 41:869-876.
24. van de Loo FA, Joosten LA, van Lent PL, Arntz OJ, van den Berg WB. Role of interleukin-1, tumor necrosis factor alpha, and interleukin-6 in cartilage proteoglycan metabolism and destruction. Effect of in situ blocking in murine antigen- and zymosan-induced arthritis. Arthritis Rheum 1995; 38:164-172.
25. Cancedda R, Descalzi Cancedda F, Castagnola P. Chondrocyte differentiation. Int Rev Cytol 1995; 159:265-358.
26. van der Eerden BC, Karperien M, Gevers EF, Lowik CW, Wit JM. Expression of Indian hedgehog, parathyroid hormone-related protein, and their receptors in the postnatal growth plate of the rat: evidence for a locally acting growth restraining feedback loop after birth. J Bone Miner Res 2000; 15:1045-1055.
27. Lanske B, Karaplis AC, Lee K, Luz A, Vortkamp A, Pirro A, Karperien M, Defize LH, Ho C, Mulligan RC, Abou-Samra AB, Juppner H, Segre GV, Kronenberg HM. PTH/PTHrP receptor in early development and Indian hedgehog-regulated bone growth. Science 1996; 273:663-666.
28. Gerstenfeld LC, Shapiro FD. Expression of bone-specific genes by hypertrophic chondrocytes: implication of the complex functions of the hypertrophic chondrocyte during endochondral bone development. J Cell Biochem 1996; 62:1-9.
29. Amizuka N, Henderson JE, Hoshi K, Warshawsky H, Ozawa H, Goltzman D, Karaplis AC. Programmed cell death of chondrocytes and aberrant chondrogenesis in mice homozygous for parathyroid hormone-related peptide gene deletion. Endocrinology 1996; 137:5055-5067.
30. Schipani E, Lanske B, Hunzelman J, Luz A, Kovacs CS, Lee K, Pirro A, Kronenberg HM, Juppner H. Targeted expression of constitutively active receptors for parathyroid hormone and parathyroid hormone-related peptide delays endochondral bone formation and rescues mice that lack parathyroid hormone-related peptide. Proc Natl Acad Sci U S A 1997; 94:13689-13694.
31. Ishikawa Y, Genge BR, Wuthier RE, Wu LN. Thyroid hormone inhibits growth and stimulates terminal differentiation of epiphyseal growth plate chondrocytes. J Bone Miner Res 1998; 13:1398-1411.
32. Chung UI, Lanske B, Lee K, Li E, Kronenberg H. The parathyroid hormone/parathyroid hormone-related peptide receptor coordinates endochondral bone development by directly controlling chondrocyte differentiation. Proc Natl Acad Sci USA 1998; 95:13030-13035.
33. Sakou T, Onishi T, Yamamoto T, Nagamine T, Sampath T, Ten Dijke P. Localization of Smads, the TGF-beta family intracellular signaling components during endochondral ossification. J Bone Miner Res 1999; 14:1145-1152.
34. Alvarez J, Balbin M, Santos F, Fernandez M, Ferrando S, Lopez JM. Different bone growth rates are associated with changes in the expression pattern of types II and X collagens and collagenase 3 in proximal growth plates of the rat tibia. J Bone Miner Res 2000; 15:82-94.
35. Chung UI, Schipani E, McMahon AP, Kronenberg HM. Indian hedgehog couples chondrogenesis to osteogenesis in endochondral bone development. J Clin Invest 2001; 107:295-304.
36. Gerber HP, Vu TH, Ryan AM, Kowalski J, Werb Z, Ferrara N. VEGF couples hypertrophic cartilage remodeling, ossification and angiogenesis during endochondral bone formation. Nat Med 1999; 5:623-628.
37. Carlevaro MF, Cermelli S, Cancedda R, Descalzi Cancedda F. Vascular endothelial growth factor (VEGF) in cartilage neovascularization and chondrocyte differentiation: auto-paracrine role during endochondral bone formation. J Cell Sci 2000; 113:59-69.
38. Engsig MT, Chen QJ, Vu TH, Pedersen AC, Therkidsen B, Lund LR, Henriksen K, Lenhard T, Foged NT, Werb Z, Delaisse JM. Matrix metalloproteinase 9 and vascular endothelial growth factor are essential for osteoclast recruitment into developing long bones. J Cell Biol 2000; 151:879-889.
39. Auphan N, DiDonato JA, Rosette C, Helmbeerg A, Karin M. Immunosuppression by glucocorticoids: Inhibition of NF-kB activity through induction of IkB synthesis. Science 1995; 270:286-290.
40. Sadowski T, Steinmeyer J. Effects of non-steroidal antiinflammatory drugs and dexamethasone on the activity and expression of matrix metalloproteinase-1, matrix metalloproteinase-3 and tissue inhibitor of metalloproteinase-1 by bovine articular chondrocytes. Osteoarthritis Cartilage 2001; 9:423-431.

Journal of Musculoskeletal Research, Vol. 6, No. 2 (2002) 63–71

ORIGINAL ARTICLES

TUMOR NECROSIS FACTOR-α CONVERTING ENZYME EXPRESSION IN THE JOINTS OF RHEUMATOID ARTHRITIS PATIENTS

Koichiro Takahi*, Tetsuya Tomita†, Takanobu Nakase, Motoharu Kaneko, Hiroshi Takano, Akira Myoui, Jun Hashimoto, Takahiro Ochi and Hideki Yoshikawa

Department of Orthopedic Surgery,
Osaka University Graduate School of Medicine, Osaka, Japan
**ktakahi@athena.ocn.ne.jp*
†*tomita@ort.med.osaka-u.ac.jp*

Received November 1, 2001; Accepted January 2, 2002

ABSTRACT

The purpose of this study is to investigate the expression of tumor necrosis factor-α converting enzyme (TACE) in the synovium and subchondral bone region of patients with rheumatoid arthritis (RA) and to determine the contribution of the enzyme to the pathogenesis of RA.

Joint tissues were obtained during total knee arthroplasty from patients with RA and osteoarthritis (OA). The expression of TACE and TNF-α mRNA was detected by *in situ* hybridization. Characterization of TACE expressing cells was performed by immunohistochemistry using serial sections.

We found that TACE mRNA was expressed in both synovium and subchondral bone region and co-localized with TNF-α mRNA in RA. On the other hand, TACE mRNA expression was scarcely detectable in OA samples. TACE was expressed in mononuclear cells, such as CD3 and CD14 positive cells in RA samples.

In conclusion, the expression of TACE is up-regulated in the rheumatoid synovium and subchondral bone region, and the results in this study demonstrate that TACE may be involved and play a role in the pathogenesis of RA.

Keywords: Rheumatoid arthritis; Tumor necrosis factor-α converting enzyme; Tumor necrosis factor-α.

Correspondence to: Dr. Tetsuya Tomita, Department of Orthopaedic Surgery, Osaka University Graduate School of Medicine, 2-2 Yamada-oka, Suita, Osaka 565-0871, Japan.

INTRODUCTION

Rheumatoid arthritis (RA) is a common autoimmune disease characterized by chronic inflammation of synovial joints and subsequent progressive destruction of cartilage and bone. Although the pathomechanisms of RA have not been fully elucidated, inflammatory cytokines and tissue damaging molecules are thought to play important roles.[12, 13, 17]

Tumor necrosis factor-alpha (TNF-α) is a major immunomodulatory and proinflammatory cytokine that is highly up-regulated in RA and may play an important role in its pathogenesis.[2, 6, 12, 13, 17] Several experimental and clinical trials have shown the effectiveness of blocking TNF-α, as well as the pivotal role of TNF-α in RA.[11, 24, 43] TNF-α is mainly produced by synovial macrophages in the RA synovium, where it stimulates fibroblast proliferation and lymphocyte activation.[9, 29] Joint destruction is a serious problem that accompanies RA, but its pathological mechanism has not been elucidated. The potential of TNF-α as a potent bone-resorbing agent has recently been recognized and it may play a major role in bone and cartilage destruction in RA.[4, 18, 22] Both local and systemic effects of TNF-α are thought to be important in these processes.

TNF-α is synthesized as a membrane-anchored precursor, then its soluble form is released into the extracellular space by limited proteolysis. The proteinase responsible for this cleavage, called TACE (TNF-α converting enzyme) or ADAM (a disintegrin and metalloproteinase domain) 17 has recently been identified.[5, 28]

The inflammatory activated synovium plays an important role in the pathogenesis of joint destruction associated with RA. Several investigators have recently demonstrated that the subchondral bone marrow also plays an important role in joint destruction associated with RA.[14, 21, 30, 32, 35-39] We detected the hyperplasia of subchondral bone marrow cells, as well as the expression of proinflammatory cytokines such as TNF-α and IL-1β and proteinases such as MMP-9, cathepsins B, K and L in subchondral bone region of joints in patients with RA. We concluded that these molecules might contribute to the joint destruction associated with RA.[21]

TACE is a key enzyme in the process of secreting soluble type TNF-α but few reports have described the role of TACE in arthritis, especially its expression in subchonodral bone region of joint destruction in RA.[1, 31, 33] The present study examines TACE expression in the synovium and subchondral bone regions of destroyed joints from patients with RA.

MATERIALS AND METHODS

Patients and Samples

Joint tissues containing synovium and subchondral bone were obtained from 7 patients with RA during total knee arthroplasty at Department of Orthopaedic Surgery Osaka University Medical School. All patients fulfilled the American College of Rheumatology revised criteria for RA[3] and gave written informed consent to fully participate in the study. The average age was 57.5 years old and average disease duration was 12 years. As controls, tissue specimens were obtained from 4 patients with osteoarthritis (OA), who averaged 54 years of age.

Tissue Preparation

Sample tissues were prepared as described.[21] They were fixed in 4% paraformaldehyde in phosphate-buffered saline (PBS; pH 7.4), decalcified in 20% EDTA, then dehydrated through an ethanol series and embedded in paraffin. Sections of 5 μm in thickness were cut using a microtome and were prepared for histological investigation including *in situ* hybridization, hematoxylin-eosin (HE) staining and immunohistochemistry.

Antibodies

Antibodies specific for T cells (anti CD-3; Dako, Glostrup, Denmark), monocytes/macrophages (CD14; Santa Cruz Biochemistry, SA) and fibroblasts (prolyl-4 hydroxylase, Fuji Chemical, Toyama, Japan) were used for immunohistochemistry. Negative controls were isotype-matched immunoglobulins.

Preparation of Probes

Digoxigenin-labeled single strand RNA probes were prepared for *in situ* hybridization using DIG (digoxigenin) RNA Labeling Kits (Boehringer Mannheim Biochemica, Mannheim, Germany) as described.[21] To generate human TNF-α probes, a 0.707 kb fragment of human TNF-α cDNA was subcloned into the pGEM-T plasmid. The plasmid was either linearized with Sac II and transcribed by SP6 RNA polymerase to generate an antisense probe or linearized with Spe I and transcribed by T7 to generate a sense probe. To generate human TACE probes, a 0.733 kb fragment of human TACE cDNA was subcloned into the pGEM-T plasmid. The plasmid was either linearized with Sal I and transcribed by T7 RNA polymerase to generate an antisense probe or linearized with Sac II and transcribed by SP6 to generate a sense probe.

In Situ Hybridization

Hybridization proceeded as described in Ref. 21 before. Briefly, after a routine treatment, each section was covered by 50 μl of hybridization solution contained approximately 0.5 mg/ml of RNA probe and incubated at 50°C for 16 hours. The slides were briefly washed in 5XSSC (1XSSC = 0.15 M NaCl, 0.015 M sodium citrate), followed by 50% formamide in 2XSSC for 30 minutes at 50°C. RNase A digestion (10mg/ml) proceeded at 37°C for 30 minutes, then the slides were washed. Hybridized probes were detected using a Nucleic Acid Detection Kit (Boehringer Mannheim Biochemica) according to the manufacturer's instructions.

Immunohistochemistry

A routine immunohistochemistry technique was used as described in Ref. 21 before. Tissue sections were deparaffinized and immunohistochemistry was performed using the streptavidin-peroxidase method with Histofine SAB-PO kits (Nichirei, Tokyo, Japan). The color reaction was performed using the substrate reagent 3,3'-diaminobenzidine tetrahydrochloride (Dojindo, Tokyo, Japan). Finally, the slides were counterstained with hematoxylin, dehydrated in a graded ethanol series and mounted.

The approximate number of positive cells was estimated in both synovium and subchondral bone region. The percentage of cells positively stained with antibodies in randomly chosen area was calculated for each section and average was shown.

RESULTS

TACE and TNF-α mRNA Expression in Destroyed RA Joints

In HE staining, all RA specimens contained the inflammatory synovium with many infiltrating cells [Fig. 1(A)]. The subchondral bone region was also characterized by cellular aggregation, extensive erosion of the subchondral plate and cartilage by cell-rich inflammatory tissue [Fig. 1(E)]. Particular cartilage destruction was evident in OA specimens, but the amount of cellular infiltration in both synovium and bone marrow was low [Fig 1(I)]. *In situ* hybridization showed that expression of TNF-α mRNA [Figs. 1(B) and (F)] and that of TACE gene [Figs. 1(C), (D), (G) and (H)] shared certain similarities. These genes were expressed in both

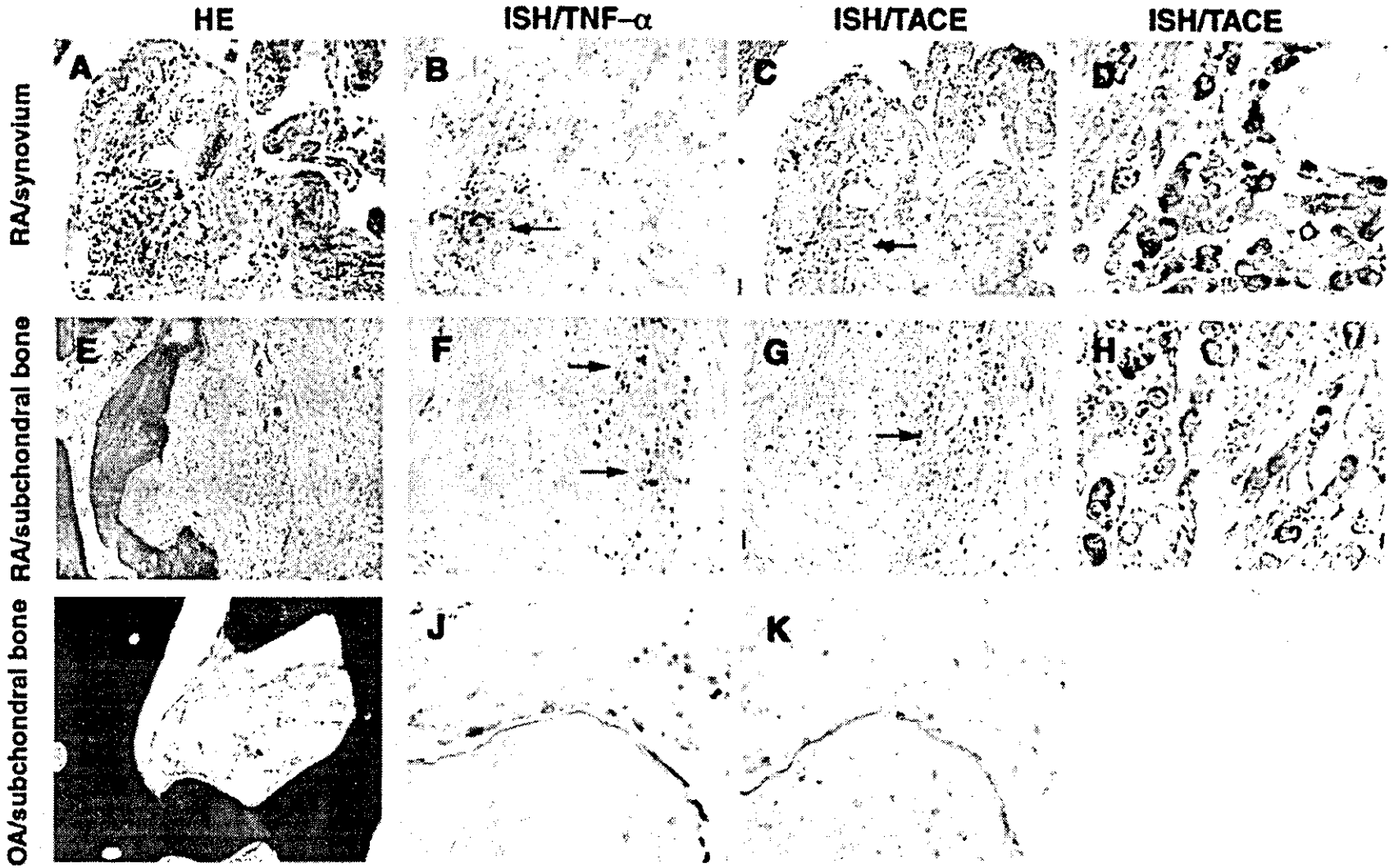

Fig. 1 TACE mRNA expression in damaged RA joint. Histological analysis of RA (A, E) and OA (I) specimens stained with hematoxylin and eosin (HE). RA specimens: regions of TACE mRNA expression were characterized by cell aggregates in the synovium (A) and in the subchondral bone region, where subchondral plate erosion by cell-rich inflammatory tissue was observed (E). OA specimen: fewer infiltrating bone marrow cells and no significant erosion of subchondral bone plate (I). *In situ* hybridization shows TNF-α (B, F) and TACE (C, D, G, H) mRNA expression in both synovium and subchondral bone region of RA joint. These genes were abundant in areas of mononuclear cell (arrows) accumulation where less TNF-α and TACE mRNA were expressed in OA specimen (J, K). (A–D, synovium of RA; E–H, subchondral bone region of RA; I–K, subchondral bone region of OA. Original magnification × 100 in A–C, F, G, J and K; × 400 in D and H; × 40 in E and I.)

the proliferative synovium [Figs. 1(B), (C) and (D)] and subchondral bone region [Figs. 1(F), (G) and (H)] of all RA joint. The TACE genes were clustered especially in areas of mononuclear cell accumulation. Serial sections showed that TNF-α mRNA and TACE gene were expressed in the corresponding areas of RA specimens, while the expression of these genes was negligible in OA specimens [Figs. 1(J) and (K)].

Characterization of Cells Expressing TACE mRNA

To characterize the cells expressing TACE mRNA, immunohistochemistry for CD3, CD14 and prolyl-4-hydroxylase (PH) was performed using serial sections. CD3 and CD14-positive cells should be T cells and monocytes/macrophages respectively, and were detected in both the synovium and the subchondral bone region [Figs. 2(A)and (C)]. In synovium, the percentages of CD3 or CD14-positive cells in mononuclear cells were about 25% and 18% respectively, and these cells had a tendency to aggregate like folicles, where TACE mRNA was mainly expressed. PH-positive cells were considered to be fibroblasts, but in these cells TACE mRNA was scarcely detected. In subchondral bone region, CD3 or CD14-positive cells were also detected and the clumps lay scattered. Percentages of CD3- or CD14-positive cells in mononuclear cells were about 15% and 8%, respectively. Some areas where these cells detected coincided with that TACE gene were expressed [Figs. 2(B) and (D)]. About 20% of mononuclear cells in the subchondral bone region and in the synovium were PH-positive. However, the localization of cells expressing TACE and PH differed (data not shown). TACE mRNA was also detected in cubic mononuclear cells lining the bone surface [Figs. 2(E) and (F)]. These cells were morphologically similar to osteoblasts and 70–80% of them expressed TACE mRNA.

DISCUSSION

TACE is a metalloproteinase that can process pro TNF-α to its soluble form and it has been identified in several cell types in some tissues.[5, 8, 28, 34] Both the membrane-anchored form and soluble form of TNF-α are considered to play an important role in inflammatory status.[15, 16, 40]

Several investigators including our group revealed abnormalities in subchondral bone region of RA and subchondral bone region as well as inflammatory synovium is considered to play an important role in the joint destruction of RA.

The present study revealed that TACE mRNA is highly expressed in affected joint with RA. Cells expressing TACE mRNA were detected in the subchondral bone region as well as in the synovium, and TACE and TNF-α genes were expressed in corresponding areas. On the other hand, few cells were positive for TACE and TNF-α mRNA in OA specimens. These findings suggest that cells producing TNF-α might simultaneously expressed TACE in RA tissues. Several studies have reported high concentration soluble form of TNF-α in the synovial fluid and serum of RA patients and TACE must play a role in these statuses. [19, 20, 43]

Our histological analyses demonstrated that TACE mRNA was expressed on some mononuclear cells, namely CD14-positive monocytes/macrophages, CD3-positive T cells and osteoblasts and number of TACE positive cells was significantly increased in RA compared with OA joints. Monocytes/macrophages constitute on major group of cells that maintains inflammation in RA joints.[12, 26, 29, 41] The present study found aggregates of these cells in the synovium and subchondral bone region from RA patients.

We also showed that some T cells expressed TACE mRNA in both the synovium and the subchondral region. In addition to the ability to bring about an immuno-reaction that is thought to play a pivotal role in the initiation of RA, T cells also seem to contribute to inflammation and joint

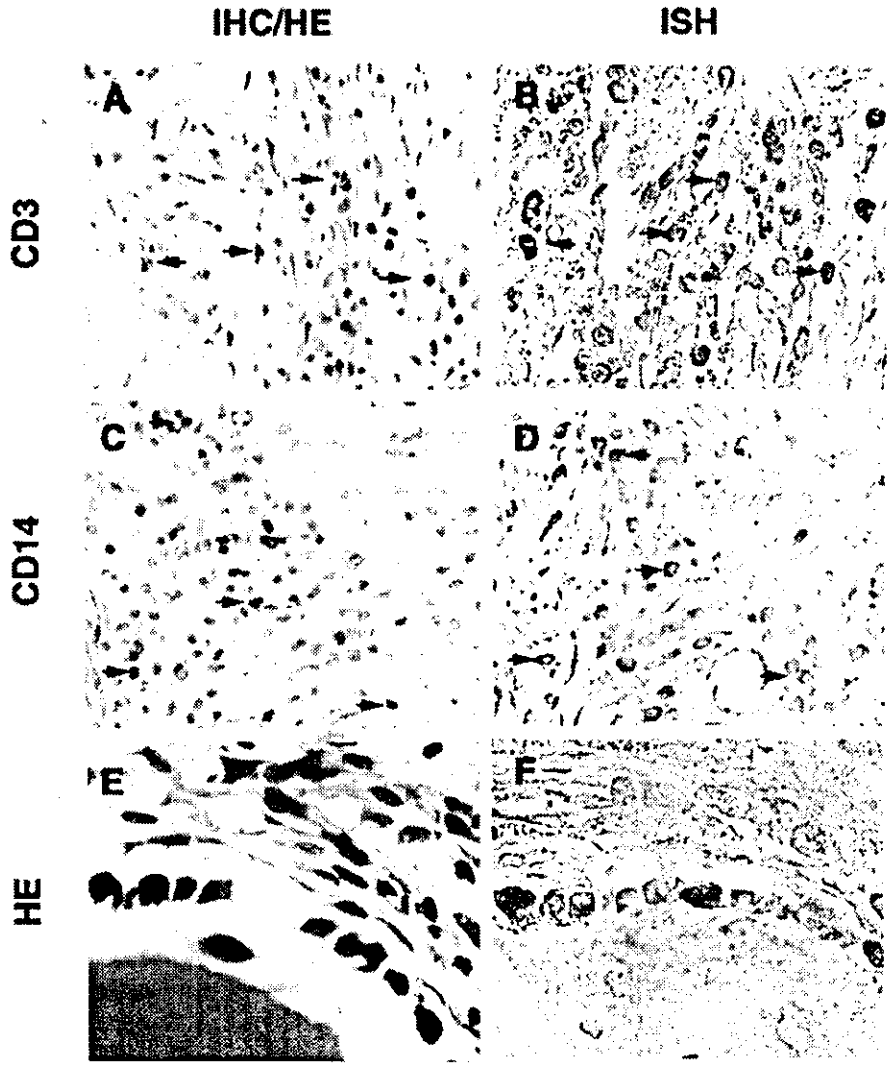

Fig. 2 Characterization of cells expressing TACE in damaged RA joints. Immunohistochemistry shows aggregated CD3 and CD14-positive cells (arrows in A and C). *In situ* hybridization demonstrates that areas of TACE-positive cell aggregation partly corresponded with those of CD3 and CD14-positive cell aggregation (arrows in B and D). Cubic mononuclear cells lining the bone surface were considered to be osteoblasts by HE staining (E) and these cells also expressed TACE mRNA (F). (Original magnification × 200 in A–D; × 400 in E and F.)

destruction of RA.[22,23,27,29] In these processes, TACE may be involved.

Fibroblasts in the synovium constitute one of the major types of cells producing TNF-α.[26,29] We examined the fibroblasts by immunohistochemistry using anti-PH. In the synovium and subchondral bone, 15–30% of mononuclear cells was stained with anti-PH antibody, but these did not correspond to TACE-positive cells. Further investigation is now undergoing to clarify this issue including identify other cell types which express TACE.

The result of our study corresponded with previous report[31] and for the first time demonstrated the increased expression of TACE mRNA in subchondral bone region of RA.

Indeed, little is known about TACE upregulation except for the TACE-mediated ectodomain shedding of several proteins is increased by stimulation of cell with some molecules.[10] Furthermore, TACE is known to be a mediator of TNF receptor II secretion which has an inhibitory effects on TNF-α action.[31] But our findings lead us to consider that TACE is likely to play a role in inflammation and/or destruction in the subchondral bone region and synovium by several effects, such as activation of the Notch pathway, and TRANCE shedding, in addition to the cleavage of pro-TNF-α. [7, 25]

CONCLUSION

The increased TACE expression in subchondral bone region as well as synovium of RA was observed and such a phenomenon might be closely related to the pathogenesis of RA. Further investigation would reveal that TACE has potential as a therapeutic target that could prevent the inflammation and joint destruction associated with RA.

ACKNOWLEDGMENTS

The authors would like to thank Kaori Izumi, Fumi Tamaki, Kanae Asai and Shoko Kuroda for excellent technical assistance. This research was supported by a grant from the Organization for Pharmaceutical Safety and Research and by a Grant-in-Aid for Scientific Research from Ministry of Education, Science and Culture, Japan.

References

1. Amin AR. Regulation of tumor necrosis factor-alpha and tumor necrosis factor converting enzyme in human osteoarthritis. *Osteoarthritis Cartilage* 7(4):392–394, 1999.
2. Arend WP, Dayer JM. Inhibition of the production and effects of interleukin-1 and tumor necrosis factor alpha in rheumatoid arthritis. *Arthritis Rheum* 38(2):151–160, 1995.
3. Arnett FC, Edworthy SM, Bloch DA, McShane DJ, Fries JF, Cooper NS, Healey LA, Kaplan SR, Liang MH, Luthra HS. Medsger TA, Mitchell DM, Neustadt DH, Pinals RS, Schaller JG, Sharp JT, Wilder RL, Hunder GG. The American Rheumatism Association 1987 revised criteria for the classification of rheumatoid arthritis. *Arthritis Rheum* **31**(3):315–24, 1988.
4. Azuma Y, Kaji K, Katogi R, Takeshita S, Kudo A. Tumor necrosis factor-alpha induces differentiation of and bone resorption by osteoclasts. *J Biol Chem* **18;275**(7): 4858–4864, 2000.
5. Black RA, Rauch CT, Kozlosky CJ, Peschon JJ, Slack JL, Wolfson MF, Castner BJ, Stocking KL, Reddy P, Srinivasan S, Nelson N, Boiani N, Schooley KA, Gerhart M, Davis R, Fitzner JN, Johnson RS, Paxton RJ, March CJ, Cerretti DP. A metalloproteinase disintegrin that releases tumor-necrosis factor-alpha from cells. *Nature* **385**(20):729–733, 1997.
6. Brennan FM, Maini RN, Feldmann M. Role of pro-inflammatory cytokines in rheumatoid arthritis. *Springer Semin Immunopathol* **20**(1–2):133–147, 1998.
7. Brou C, Logeat F, Gupta N, Bessia C, LeBail O, Doedens JR, Cumano A, Roux P, Black RA, Israel A. A novel proteolytic cleavage involved in Notch signaling: The role of the disintegrin-metalloprotease TACE. *Mol Cell* **5**(2):207–216, 2000.
8. Buxbaum JD, Liu KN, Luo Y, Slack JL, Stocking KL, Peschon JJ, Johnson RS, Castner BJ, Cerretti DP, Black RA. Evidence that tumor necrosis factor alpha converting enzyme is involved in regulated alpha-secretase cleavage of the Alzheimer amyloid protein precursor. *J Biol Chem* **23;273**(43):27765–27767, 1998.
9. Chu CQ, Field M, Feldmann M, Maini RN. Localization of tumor necrosis factor alpha in synovial tissues and at the cartilage-pannus junction in patients with rheumatoid arthritis. *Arthritis Rheum* **34**(9):1125–1132, 1991.
10. Doedens JR, Black RA. Stimulation-induced down-regulation of tumor necrosis factor-alpha converting enzyme. *J Biol Chem* **275**(19):14598–14607, 2000.
11. Elliott MJ, Maini RN, Feldmann M, Kalden JR, Antoni C, Smolen JS, Leeb B, Breedveld FC, Macfarlane JD, Bijl H, Woody JM. Randomised double-blind comparison of chimeric monoclonal antibody to tumour necrosis factor alpha (cA2) versus placebo in rheumatoid arthritis. *Lancet* **22;344**(8930):1105–1110, 1994.
12. Feldmann M, Brennan FM, Maini RN. Role of cytokines in rheumatoid arthritis. *Ann Rev Immunol*, Vol. 14, Palo Alto, Annual Reviews, 1996, pp. 397–440.
13. Feldmann M, Brennan FM, Maini RN. Rheumatoid arthritis. *Cell* **85**(3):307–310, 1996.
14. Fujii K, Tsuji M, Tajima M. Rheumatoid arthritis: A synovial disease? *Ann Rheum Dis* **58**(12): 727–730, 1999.

15. Gearing AJ, Beckett P, Christodoulou M, Churchill M, Clements J, Davidson AH, Drummond AH, Galloway WA, Gilbert R, Gordon JL. Leber TM, Mangan M, Miller K, Nayee P, Owen K, Patel S, Thomas W, Wells G, Wood LM, Wooley K. Processing of tumour necrosis factor-alpha precursor by metalloproteinases. *Nature* **18;370**(6490):555–557, 1994.
16. Grell M, Douni E, Wajant H, Lohden M, Clauss M, Maxeiner B, Georgopoulos S, Lesslauer W, Kollias G, Pfizenmaier K, Scheurich P. The transmembrane form of tumor necrosis factor is the prime activating ligand of the 80 kDa tumor necrosis factor receptor. *Cell* **1;83**(5):793–802, 1995.
17. Goldring SR, Gravallese EM. Pathogenesis of bone erosions in rheumatoid arthritis. *Curr Opin Rheumatol* **12**(3):195–199, 2000.
18. Hofbauer LC, Heufelder AE. The role of osteoprotegerin and receptor activator of nuclear factor kappaB ligand in the pathogenesis and treatment of rheumatoid arthritis. *Arthritis Rheum* **44**(2):253–259, 2001.
19. Hopkins SJ, Humphreys M, Jayson MI. Cytokines in synovial fluid. I. The presence of biologically active and immunoreactive IL-1. *Clin Exp Immunol* **72**(3):422–427, 1988.
20. Hopkins SJ, Meager A. Cytokines in synovial fluid: II. The presence of tumour necrosis factor and interferon. *Clin Exp Immunol* **73**(1):88–92, 1988.
21. Kaneko M, Tomita T, Nakase T, Ohsawa Y, Seki H, Takeuchi E, Takano H, Shi K, Takahi K, Kominami E, Uchiyama Y, Yoshikawa H, Ochi T. Expression of proteinases and inflammatory cytokines in subchondral bone regions in the destructive joint of rheumatoid arthritis. *Rheumatology (Oxford)* **40**(3):247–255, 2001.
22. Kobayashi K, Takahashi N, Jimi E, Udagawa N, Takami M, Kotake S, Nakagawa N, Kinosaki M, Yamaguchi K, Shima N, Yasuda H, Morinaga T, Higashio K, Martin TJ, Suda T. Tumor necrosis factor alpha stimulates osteoclast differentiation by a mechanism independent of the ODF/RANKL-RANK interaction. *J Exp Med* **17;191**(2):275–286, 2000.
23. Kong YY, Feige U, Sarosi I, Bolon B, Tafuri A, Morony S, Capparelli C, Li J, Elliott R, McCabe S, Wong T, Campagnuolo G, Moran E, Bogoch ER, Van G, Nguyen LT, Ohashi PS, Lacey DL, Fish E, Boyle WJ, Penninger JM. Activated T cells regulate bone loss and joint destruction in adjuvant arthritis through osteoprotegerin ligand. *Nature* **18;402**(6759):304–309, 1999.
24. Lipsky PE, van der Heijde DM, St Clair EW, Furst DE, Breedveld FC, Kalden JR, Smolen JS, Weisman M, Emery P, Feldmann M, Harriman GR, Maini RN. Infliximab and methotrexate in the treatment of rheumatoid arthritis. Anti-Tumor Necrosis Factor Trial in Rheumatoid Arthritis with Concomitant Therapy Study Group. *N Engl J Med* **30;343**(22):1594–1602, 2000.
25. Lum L, Wong BR, Josien R, Becherer JD, Erdjument-Bromage H, Schlondorff J, Tempst P, Choi Y, Blobel CP. Evidence for a role of a tumor necrosis factor-alpha (TNF-alpha)-converting enzyme-like protease in shedding of TRANCE, a TNF family member involved in osteoclastogenesis and dendritic cell survival. *J Biol Chem* **274**(19):13613–13618, 1999.
26. MacNaul KL, Hutchinson NI, Parsons JN, Bayne EK, Tocci MJ. Analysis of IL-1 and TNF-alpha gene expression in human rheumatoid synoviocytes and normal monocytes by *in situ* hybridization. *J Immunol* **145**(12): 4154–4166, 1990.
27. Miossec P. Are T cells in rheumatoid synovium aggressors or bystanders? *Curr Opin Rheumatol* **12**(3): 181–185, 2000.
28. Moss ML, Catherine Jin SL, Milla ME, Moss ML, Jin SL, Milla ME, Bickett DM, Burkhart W, Carter HL, Chen WJ, Clay WC, Didsbury JR, Hassler D, Hoffman CR, Kost TA, Lambert MH, Leesnitzer MA, McCauley P, McGeehan G, Mitchell J, Moyer M, Pahel G, Rocque W, Overton LK, Schoenen F, Seaton T, Su JL, Warner J, Willard D, Becherer JD. Cloning of a disintegrin metalloproteinase that processes precursor tumour-necrosis factor-alpha. *Nature* **385**(20):733–736, 1997.
29. Muller-Ladner U, Gay RE, Gay S. Activation of synoviocytes. *Curr Opin Rheumatol* **12**(3):186–194, 2000.
30. Ochi T, Hakomori S, Adachi M, Owaki H, Okamura M, Ono Y, Yamasaki K, Fujimoto M, Wakitani S, Ono K. The presence of a myeloid cell population showing strong reactivity with monoclonal antibody directed to difucosyl type 2 chain in epiphyseal bone marrow adjacent to joints affected with rheumatoid arthritis (RA) and its absence in the corresponding normal and non-RA bone marrow. *J Rheumatol* **15**(11):1609–1615, 1988.
31. Ohta S, Harigai M, Tanaka M, Kawaguchi Y, Sugiura T, Takagi K, Fukasawa C, Hara M, Kamatani N. Tumor necrosis factor-alpha (TNF-alpha) converting enzyme contributes to production of TNF-alpha in synovial tissues from patients with rheumatoid arthritis. *J Rheumatol* **28**(8):1756–1763, 2001.
32. Owaki H, Ochi T, Yamasaki K, Yukawa K, Wakitani S, Okamura M, Ono K. Elevated activity of myeloid growth factor in bone marrow adjacent to joints affected by rheumatoid arthritis. *J Rheumatol* **16**(5): 572–577, 1989.
33. Patel IR, Attur MG, Patel RN, Stuchin SA, Abagyan RA, Abramson SB, Amin AR. TNF-alpha convertase enzyme from human arthritis-affected cartilage: Isolation of cDNA by differential display, expression of the

active enzyme, and regulation of TNF-alpha. *J Immunol* **160**(9): 4570–4579, 1998.
34. Satoh M, Nakamura M, Saitoh H, Satoh H, Maesawa C, Segawa I, Tashiro A, Hiramori K. Tumor necrosis factor-alpha-converting enzyme and tumor necrosis factor-alpha in human dilated cardiomyopathy. *Circulation* **99**(25):3260–3265, 1999.
35. Tanabe M, Ochi T, Tomita T, Suzuki R, Sakata T, Shimaoka Y, Nakagawa S, Ono K. Remarkable elevation of interleukin 6 and interleukin 8 levels in the bone marrow serum of patients with rheumatoid arthritis. *J Rheumatol* **21**(5):830–835, 1994.
36. Tomita T, Kashiwagi N, Shimaoka Y, Ikawa T, Tanabe M, Nakagawa S, Kawamura S, Denno K, Owaki H, Ochi T. Phenotypic characteristics of bone marrow cells in patients with rheumatoid arthritis. *J Rheumatol* **21**(9): 1608–1614, 1994.
37. Tomita T, Shimaoka Y, Kashiwagi N, Hashimoto H, Kawamura S, Lee SB, Nakagawa S, Shiho O, Hayashida K, Ochi T. Enhanced expression of CD14 antigen on myeloid lineage cells derived from the bone marrow of patients with severe rheumatoid arthritis. *J Rheumatol* **24**(3):465–469, 1997.
38. Tomita T, Takeuchi E, Toyosaki-Maeda T, Oku H, Kaneko M, Takano H, Sugamoto K, Ohzono K, Suzuki R, Ochi T. Establishment of nurse-like stromal cells from bone marrow of patients with rheumatoid arthritis: Indication of characteristic bone marrow microenvironment in patients with rheumatoid arthritis. *Rheumatology(Oxford)* **38**(9):854–863, 1999.
39. Toritsuka Y, Nakamura N, Lee SB, Hashimoto J, Yasui N, Shino K, Ochi T. Osteoclastogenesis in iliac bone marrow of patients with rheumatoid arthritis. *J Rheumatol* **24**(9):1690–1696, 1997.
40. Vassalli P. The pathophysiology of tumor necrosis factors: *Ann Rev Immunol*, Vol. 10, Palo Alto, Annual Reviews, 1992, pp. 411–452.
41. van den Berg WB, van Lent PL. The role of macrophages in chronic arthritis. *Immunobiology* **195**:614–623, 1996.
42. Williams RO, Feldmann M, Maini RN. Anti-tumor necrosis factor ameliorates joint disease in murine collagen-induced arthritis. *Proc Natl Acad Sci USA* **15;89**(20):9784–9788, 1992.
43. Yocum DE, Esparza L, Dubry S, Benjamin JB, Volz R, Scuderi P. Characteristics of tumor necrosis factor production in rheumatoid arthritis. *Cell Immunol* **122**(1): 131–145, 1989.

JOURNAL OF BONE AND MINERAL RESEARCH
Volume 17, Number 10, 2002

Continuous Inhibition of MAPK Signaling Promotes the Early Osteoblastic Differentiation and Mineralization of the Extracellular Matrix

CHIKAHISA HIGUCHI,[1,2] AKIRA MYOUI,[2] NOBUYUKI HASHIMOTO,[2] KOHJI KURIYAMA,[1,2] KIYOKO YOSHIOKA,[1] HIDEKI YOSHIKAWA,[2] and KAZUYUKI ITOH[1]

ABSTRACT

We screened the small molecule compounds that stimulate osteogenesis by themselves or promote bone morphogenetic protein (BMP)–induced bone formation. We found that a specific inhibitor for MAPK/extracellular signal–regulated kinase kinase (MEK)-1, promoted the early osteoblastic differentiation and mineralization of extracellular matrix (ECM) in C2C12 pluripotent mesenchymal cells treated with recombinant human BMP-2 (rhBMP-2) and MC3T3-E1 preosteoblastic cells. ALP activity was synergistically increased by the treatment with a specific MEK-1 inhibitor PD98059 and rhBMP-2 in both cell lines. Twenty-five micromolar PD98059 promoted mineralization of ECM in rhBMP-2–treated C2C12 cells and MC3T3-E1 cells. In contrast, PD98059 reduced osteocalcin (OCN) secretion and its transcriptional level in rhBMP-2–treated C2C12 cells but increased its secretion and mRNA level in MC3T3-E1 cells. Stable expression of a dominant-negative MEK-1 mutant in C2C12 cells represented high ALP activity and low osteocalcin production in the presence of rhBMP-2, while a constitutively active mutant of MEK-1 attenuated both of them. Together, our results indicated that BMP-2–induced mineralization of ECM of pluripotent mesenchymal stem cells and preosteoblastic cells could be controlled by a fine tuning of the MAPK signaling pathway. Further, MEK-1 inhibitors would be useful for the promotion of bone formation, for instance, the treatments for delayed fracture healing or advance of localized osteoporotic change after fracture healing. (J Bone Miner Res 2002;17:1785–1794)

Key words: MAPK, mineralization, bone morphogenetic protein, osteoblastic differentiation, inhibitor

INTRODUCTION

ORTHOPEDIC SURGEONS often have opportunities to manage the fractures of osteoporotic bones, especially the distal radius and proximal femur of elderly women. Several complications may occur during the treatment, for instance, the nonunion of fracture site, advance of localized osteoporotic change around the fracture site because of the prolonged period of treatment, etc. To overcome these problems, we screened the small molecule compounds that induced osteogenesis by themselves or promoted bone morphogenetic protein (BMP)–induced bone formation. The final goal of our study would be clinical application of them. Here, we found that a specific inhibitor for MAPK/extracellular signal–regulated kinase kinase (MEK)-1 promoted mineralization of the extracellular matrix (ECM) formed by mesenchymal pluripotent cells and preosteoblastic cells in vitro.

BMPs are members of the transforming growth factor (TGF)-β superfamily and play critical roles in osteogenesis.

The authors have no conflict of interest.

[1]Department of Biology, Osaka Medical Center for Cancer and Cardiovascular Diseases, Higashinari-ku, Osaka, Japan.
[2]Department of Orthopedic Surgery, Osaka University Medical School, Suita, Osaka, Japan.

They induce ectopic bone formation in vivo when implanted in muscular tissue[1] and modulate the osteoblastic differentiation of mesenchymal stem cells in vitro.[2-5] The molecular mechanisms of the osteoblastic differentiation by BMP-2 were well characterized.[6-10] BMP-2 is thought to exert their biological function by interacting with two types of transmembrane serine/threonine kinase receptors. These BMP receptors phosphorylate transcriptional factors Smad1, -5, and -8. The phosphorylated Smads bind to Smad4 following the complex translocates into the nucleus and regulates the transcriptional activation of genes related to the osteoblastic differentiation resulting in bone formation. A clinical trial of recombinant human BMP-2 (rhBMP-2) has been done, but a huge amount of rhBMP-2 was required for bone formation to the treatment of fracture, bone defect, spinal fusion, etc.[11,12] Thus, small molecule compounds, which synergistically reinforce the effects of rhBMP-2 on bone formation or induce osteogenesis by themselves, would be useful for its clinical application. Simvastatin, a 3-hydroxy-3-methylglutaryl coenzyme A (HMG CoA) reductase inhibitor, was first reported to be one candidate that promoted osteogenesis.[13,14]

The MEK/MAPK signaling pathway plays significant roles in cell proliferation and differentiation. This signaling also affects the osteoblastic differentiation in mesenchymal cells. Takeuchi et al. showed that integrin activation by ECM induced the activation of MAPK, which is necessary for the osteoblastic differentiation of MC3T3-E1 preosteoblasts.[15] Jaiswal et al. showed that the osteoblastic differentiation by glucocorticoid dexamethasone of adult human mesenchymal stem cells was inhibited by MEK inhibition.[16] In contrast, Kertzschmar suggested that the activation of MAPK inhibited BMP signaling by phosphorylating the linker region between the Mad homology (MH) 1 domain and MH2 domain of Smad1 and inhibiting nuclear translocation of this protein.[17] In addition, it has been reported that MAPK activation down-regulated type I collagen gene expression in MC3T3-E1 cells.[18] Therefore, the involvement of the MAPK signaling pathway on osteoblastic differentiation is somewhat controversial.

Here, we reported the effects of long-lasting alteration in MAPK signaling on the osteoblastic differentiation of mesenchymal cell lines using a specific MEK-1 inhibitor and stable expression of constitutively active or dominant-negative MEK-1 mutant as assessed by ALP activity, osteocalcin (OCN) secretion, their transcriptional levels, and a mineralized nodule.

MATERIALS AND METHODS

Cell culture

C2C12 pluripotent mesenchymal cells and MC3T3-E1 preosteoblastic cells were purchased from Riken Cell Bank (Tsukuba, Japan). C2C12 cells were cultured in DMEM supplemented with 10% FBS (Equitech-bio, Kerrville, TX, USA) at 37°C in a humidified atmosphere of 5% CO_2 and MC3T3-E1 cells in α-minimum essential medium (α-MEM) containing 10% FBS. All mediums were purchased from Invitrogen Life Technologies (Tokyo, Japan).

For each assay, C2C12 cells and stable transfectants were seeded at 1×10^4 cells/cm^2, and MC3T3-E1 cells were seeded at 2×10^4 cells/cm^2. Twenty-four hours after plating, the medium was replaced by the new medium containing 10% FBS in the absence or presence of rhBMP-2 (generous gift from the Genetics Institute, Cambridge, MA, USA, and Yamanouchi pharmaceutical Co., Tokyo, Japan) and MEK-1 inhibitor PD98059 (New England Biolabs, Inc., Beverly, MA, USA).

Constructs and transfection

Hemagglutinin (HA)-tagged constitutively active rat MEK-1 expression vector was purchased from Upstate Biotechnology (Lake Placid, NY, USA). HA-tagged constitutively active MEK-1 cDNA was excised from the vector as a *Bam*HI/*Xho*I fragment and transferred into pcDNA3 expression vector (Invitrogen Life Technologies). HA-tagged nonactivatable (dominant-negative) MEK-1 cDNA was made by alanine substitutions of two aspartic acids in HA-tagged constitutively active MEK-1 cDNA, which were substituted in place of serine residues 218 and 222 in wild-type cDNA for its activation, using polymerase chain reaction (PCR) using appropriate primers.[19]

These plasmids and empty vectors were transfected into C2C12 cells using LipofectAMINE PLUS (Invitrogen Life Technologies) following the manufacturer's protocol and selected with 1 mg/ml of G418 sulfate (Invitrogen Life Technologies) to obtain stable transfectants. Expression of mutated protein in stable transfectants was detected by immunoblotting using anti-MEK-1 antibody and anti-HA antibody (Santa Cruz Biotechnology, Inc., Santa Cruz, CA, USA).

ALP staining and activity

C2C12 cells and MC3T3-E1 cells were treated with or without rhBMP-2 and MEK-1 inhibitor 24 h after being seeded and incubated for 3 days.

For ALP staining, cells were fixed for 15 minutes with 3.7% formaldehyde at room temperature after being washed with PBS. After the fixation, they were incubated with the mixture of nitro blue tetrazolium (NBT; Promega, Madison, WI, USA) and 5-bromo-4-chloro-3-indolyl-phosphate (BCIP; Promega) in ALP buffer (100 mM of Tris-HCl, pH 9.5, 100 mM of NaCl, and 5 mM of $MgCl_2$) for 1 h in the dark at room temperature.

To measure ALP activity, cells were washed twice with PBS and lysed in M-Per Mammalian Protein Extraction Reagent (Pierce, Rockford, IL, USA) following its protocol. ALP activity was assayed using *p*-nitrophenylphosphate as a substrate by Alkaline Phospha Test Wako (Wako Pure Chemicals Industries, Ltd., Osaka, Japan) and the protein content was measured using the bicinchoninic acid (BCA) protein assay kit (Pierce).

Transfectants were treated with or without rhBMP-2 for 3 days and ALP activity was measured as mentioned previously.

Immunofluorescence for troponin T

C2C12 cells were cultured in DMEM supplemented with 10% FBS in the absence or presence of 300 ng/ml of

rhBMP-2 and 25 μM of PD98059 on a Lab-Tek chamber slide (Nunc, Roskilde, Denmark) for 3 days. Cells were fixed with 3.7% formaldehyde for 15 minutes at room temperature and permeabilized with 0.5% Triton-X 100 in PBS. After washing the cells with PBS twice and blocking with 5% normal goat serum in 0.1% Tween 20–containing PBS (T-PBS), they were incubated for 1 h with mouse anti–troponin T (TnT) monoclonal antibody (Sigma, Tokyo, Japan) at 1:200 dilution at room temperature. The cells were washed three times with T-PBS and incubated for 30 minutes with fluorescein isothiocyanate (FITC)–conjugated anti-mouse secondary antibody at 1:200 dilution (Santa Cruz Biotechnology, Inc.). Immunofluorescence for TnT was followed by ALP staining. The cells were observed using a fluorescence microscopy IX-70 (Olympus, Tokyo, Japan) attached with a camera. The number of total TnT^+ or ALP^+ cells was counted in five microscopic fields of one experiment and the percentage of positive cells/total cells was calculated. Total number of the cells was counted over 2000 in one experiment. Three duplicated experiments were done independently.

OCN secretion

The amount of OCN secreted into the culture medium between day 4 and 6 was determined by radioimmunoassay using the mouse osteocalcin immunoradiometric assay (IRMA) kit (Immutopics, Inc., San Clemente, CA, USA). Because the MEK inhibitor showed cellular growth inhibition, OCN secretion was normalized to the total cellular protein content.

Alizarin red S staining and calcium content in mineralized nodule assay

C2C12 cells were cultured in DMEM containing 10% FBS, 50 μg/ml of ascorbic acid (Invitrogen Life Technologies), and 10 mM of β-glycerophosphate (Sigma) in the absence or presence of 300 ng/ml of rhBMP-2 and 25 μM of MEK inhibitor for 12 days for mineralized nodule assay. MC3T3-E1 cells were cultured in α-MEM containing 10% FBS and 10 mM of β-glycerophosphate in the absence or presence of 50 ng/ml of rhBMP-2 and 25 μM of PD98059 for 15 days. The medium was replaced every 3 days. For alizarin red S (Sigma) staining to detect mineralized nodules, the cells were washed with deionized water after being fixed for 15 minutes with 3.7% formaldehyde at room temperature and stained with alizarin red S at pH 6.3.

To measure calcium content of the nodule, 500 μl of 0.6N HCl was added to each well to decalcify mineralized nodules after fixation of the cells.[20] After 24 h, calcium content in the supernatant was determined using the *o*-cresolphthalein complexon color development method by the Calcium Test Wako (Wako Pure Chemicals Industries, Ltd.). Duplicated wells were used to determine the protein content.

Immunoblotting

After cells were cultured with various treatments for 3 days, they were lysed rapidly in ice with Laemmli's SDS sample buffer (62.5 mM of Tris-HCl, pH 6.8, 2% SDS, 10% glycerol, and 0.01% phenol red)[21] containing 40 mM of dithiothreitol with a cell scraper. These samples were subjected to SDS 4–20% gradient PAGE (Daiichi Pure Chemicals Co, Ltd., Tokyo, Japan) for detection of MAPK or 10% for TnT, myosin heavy chain (MHC), MyoD, and β-actin. Proteins were transferred to nitrocellulose membranes (Bio-Rad Laboratories, Inc., Hercules, CA, USA). The membranes were immunoblotted with primary antibodies in T-PBS containing 1% bovine serum albumin (BSA; Promega) overnight after 1-h blocking with T-PBS containing 3% BSA. Anti-MAPK antibody (New England Biolabs, Inc.) and anti-phosphoMAPK antibody (New England Biolabs, Inc.) were used as the primary antibody at 1:1000 dilution. Anti-TnT antibody, anti-MHC antibody (MF-20; Developmental Studies Hybridoma Bank, Iowa City, IA, USA), and anti–β-actin antibody (Chemicon International, Temecala, CA, USA) were used at 1:200. The membrane was incubated for 30 minutes with secondary antibodies (anti-rabbit or anti-mouse immunoglobulin G [IgG] Fc ALP conjugate; Promega) at 1:7500 dilution after wash for 10 minutes in T-PBS three times. Immunoreactive bands were visualized by incubation of the membrane in the mixture of NBT and BCIP in ALP buffer mentioned previously.

Phosphorylation level of MAPK

For relative estimation of phosphorylation of MAPK, the blot membrane was scanned with a GT9500 flat scanner (Epson, Tokyo, Japan) and analyzed with the National Institutes of Health (NIH) image software.

An immunoreactive band of phosphorylated p42 MAPK was distinguished from that of nonphosphorylated p42 MAPK by SDS 4–20% gradient PAGE. The standard absolute phosphorylation level of p42 MAPK was estimated using the membrane that was immunoblotted by anti-MAPK antibody as the following equation:

$$\text{standard absolute phosphorylation level of p42 MAPK} = \frac{\text{pp42 band signal}}{\text{total p42(p42 band signal + pp42 band signal)}} \times 100(\%).$$

The signal closest to 50% was used to calculate a standard absolute phosphorylation level of MAPK and avoided the interference with pp42 and p42 immunoreactive band signal when the large difference exists between these two.[22] Relative phosphorylation level was estimated from the signal of phosphorylated p42 in membrane blotted by anti–phospho-MAPK antibody, which was normalized with the signal of total p42. Each absolute phosphorylation level was estimated as the following equation:

$$\text{each phosphorylation level of p42 MAPK} = \text{standard absolute phosphorylation level of p42 MAPK} \times \text{relative phosphorylation level.}$$

RNA blot

Total RNA was extracted using TRIZOL reagent (Invitrogen Life Technologies). Ten micrograms of total RNA was

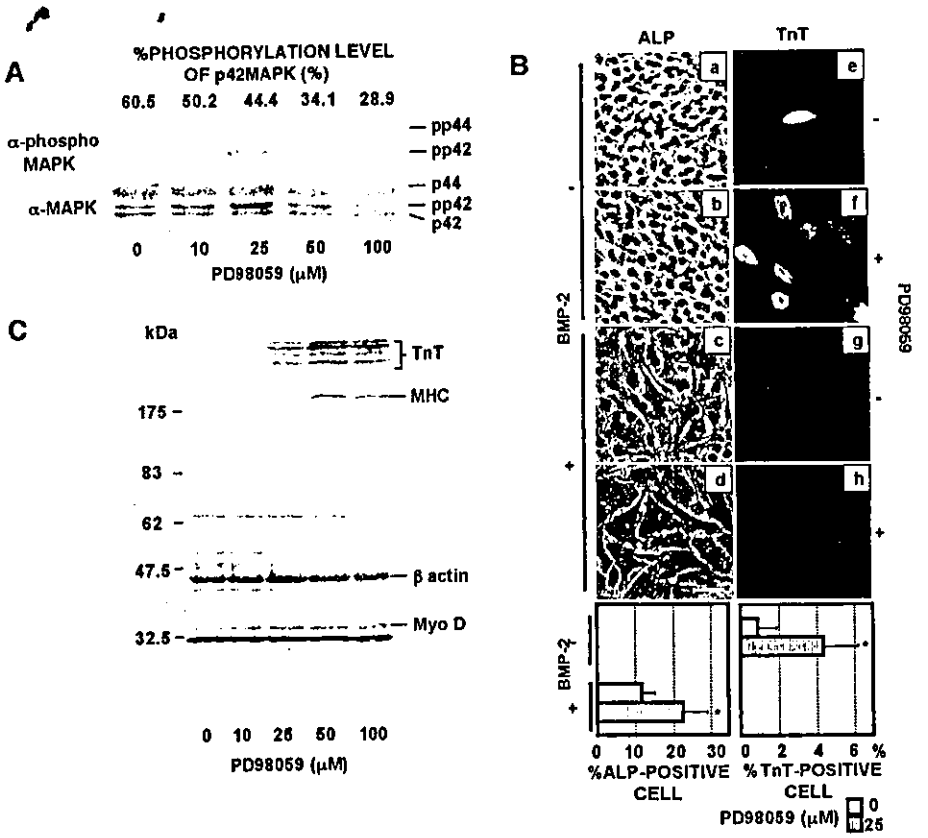

FIG. 1. Effects of the MEK-1 inhibitor PD98059 on the phosphorylation level of MAPK and the differentiation of C2C12 cells. (A) PD98059 reduced the phosphorylation level of MAPK in a dose-dependent fashion. Cells were cultured in DMEM supplemented with 10% FBS and MEK-1 inhibitor for 3 days. (B) ALP staining (a–d) and immunofluorescent staining for TnT (e–h) were carried out. In the absence of 300 ng/ml of rhBMP-2, the percentage of TnT^+ cells was increased by the treatment with PD98059 (f). In the presence of rhBMP-2, the number of ALP^+ cells was increased (d). C2C12 cells were cultured with 10% FBS in the absence or presence of 300 ng/ml of rhBMP-2 and 25 μM of PD98059 for 3 days. (C) Three myogenic marker (TnT, MHC, and MyoD) levels were increased in C2C12 cells treated with PD98059 for 3 days in a dose-dependent manner. Data showed mean ± five independent experiments. (bar = 50 μm; $*p < 0.05$ compared with PD98059-untreated control).

electrophoresed in 1% agarose-formaldehyde gels and transferred onto Hybond N^+ nylon membrane (Amersham Pharmacia Biotech, Tokyo, Japan). Twenty-five nanograms of the probes was radiolabeled with [α-^{32}P]deoxycytidine 5′-triphosphate (dCTP) using the Rediprime II DNA Labeling System (Amersham Pharmacia Biotech). The fragments of rat ALP cDNA[23] and mouse OCN cDNA[24] were used as probes. The membranes were prehybridized, hybridized using Rapid-Hyb Buffer (Amersham Pharmacia Biotech) with radioactive probes, and then washed with 2× SSC containing 0.1% SDS or 0.2× SSC containing 0.1% SDS. The hybridized blots were exposed to an imaging plate at room temperature and relative levels of mRNA were calculated by a laser scanning densitometer (Fuji BAS 2000; Fuji, Tokyo, Japan).

Statistic analysis

Data are expressed as mean ± SD in all figures. Statistical significance was analyzed by Student's *t*-test.

RESULTS

Effects of the MEK-1 inhibitor on the phosphorylation of MAPK and morphology in C2C12 pluripotent mesenchymal cells

The phosphorylation level of MAPK was reduced by the treatment with MEK-1 inhibitor PD98059 in C2C12 cells in a dose-dependent fashion (60.5 ± 8.26% to 28.9 ± 16.4% at 0–100 μM; Fig. 1A).

Morphologically, C2C12 cells revealed a spindle-shape (Fig. 1B, a and b) and expressed small amount of TnT, a myogenic marker (Fig. 1B, e) cultured in DMEM supplemented with 10% FBS in the absence of rhBMP-2. When cells were treated with 25 μM of MEK-1 inhibitor in the absence of rhBMP-2, the percentage of TnT^+ cells was increased ~4.9-fold (0.87 ± 0.97% to 4.30 ± 1.88%; Fig. 1B, e and f, lower right graph). In the presence of 300 ng/ml of rhBMP-2, the cell shape changed to polygonal (Fig. 1B, c and d). ALP^+ cells appeared, whereas TnT^+ ones disappeared (Fig. 1B, c, d, g, and h). The percentage of ALP^+ cells was increased 1.9-fold after the treatment with 25 μM of PD98059 (11.8 ± 3.34% to 22.5 ± 6.46%; Fig. 1B, c and d, lower left graph). Myogenic differentiation was also detected by the immunoblotting with TnT, MHC, and MyoD antibodies (Fig. 1C). Expression of these myogenic markers was increasing by the treatment with MEK-1 inhibitor even in the presence of 10% FBS. Together, these results indicated that the MEK-1 inhibitor PD98059 stimulated both myogenic and osteogenic differentiation of C2C12 cells.

Effects of the MEK-1 inhibitor on the rhBMP-2–induced osteoblastic differentiation in C2C12 cells

To further evaluate the effects of MEK-1 inhibitor on the osteoblastic differentiation, ALP staining was carried out to

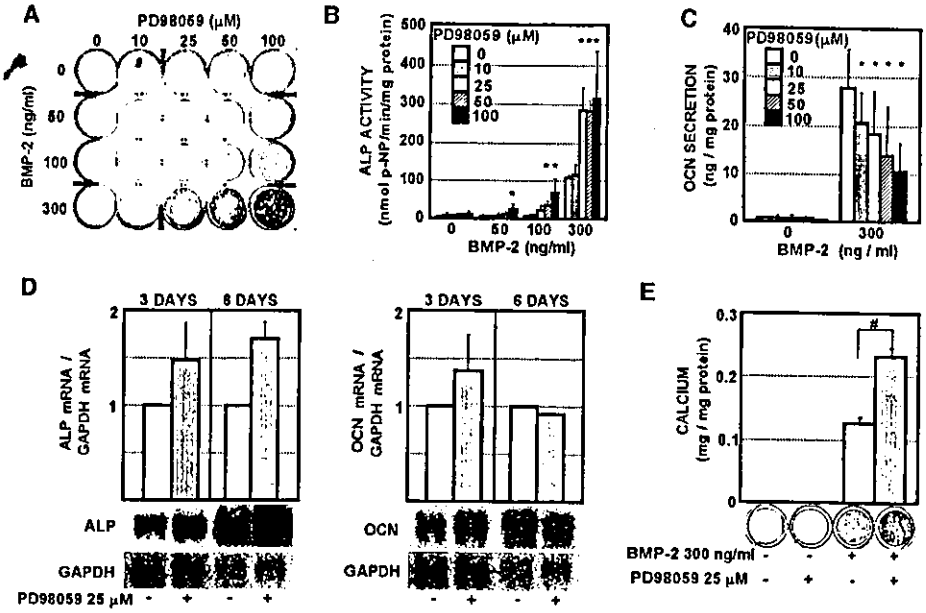

FIG. 2. Effects of PD98059 on the osteoblastic differentiation of C2C12 cells stimulated with rhBMP-2. (A) Total ALP activity in each well was synergistically increased in both rhBMP-2 and MEK-1 inhibitor in a dose-dependent fashion. The wells were stained with ALP after the culture for 3 days. (B) Effects of rhBMP-2 and PD98059 on ALP activity were synergistic. (C) OCN secreted from C2C12 cells by treatment with 300 ng/ml of rhBMP-2 was decreased in PD98059 in a dose-dependent fashion. C2C12 cells were cultured for 6 days. OCN in the culture media between day 4 and 6 was determined by radioimmunoassay. (D) mRNA levels of ALP and OCN stimulated with 300 ng/ml of rhBMP-2 were assayed by RNA blot analysis. Transcriptional level of OCN was slightly decreased after the culture for 6 days but increased after the culture for 3 days. The same amount (10 μg) of total RNA was applied to each lane. (E) The MEK-1 inhibitor promoted bone mineralization in the presence of 300 ng/ml of rhBMP-2. Calcium nodules were stained with alizarin red S. Data represent mean ± SD of three independent experiments (*$p <$ 0.05 compared with PD98059-untreated control; #$p < 0.005$).

visualize the total ALP activity of C2C12 cells (Fig. 2A). rhBMP-2 stimulated ALP activity in C2C12 cells in a dose-dependent fashion (0–300 ng/ml) and ALP activity was increasing also by the treatment with MEK-1 inhibitor in a concentration-dependent manner (0–100 μM). Figure 2B clearly shows that rhBMP-2 and PD98059 synergistically increased ALP activity. RNA blot analysis confirmed the increase of the ALP transcriptional level by the treatment with MEK-1 inhibitor after incubation for both 3 days and 6 days (Fig. 2D, left panel).

Three hundred nanograms per milliliter of rhBMP-2 induced OCN secretion from C2C12 cells. In contrast to ALP activity, OCN secretion from C2C12 cells between day 4 and 6 decreased in the presence of PD98059 in a dose-dependent fashion (0–100 μM; Fig. 2C, right five bars). OCN mRNA level also was decreased slightly by the treatment with PD98059 for 6 days, which was consistent with OCN secretion, and it was increased at day 3 (Fig. 2D, right panel).

Alizarin red S staining indicated that 300 ng/ml of rhBMP-2 induced mineralization of ECM of C2C12 cells and that the additional treatment with 25 μM of MEK-1 inhibitor enhanced the calcium deposition (Fig. 2E, panel). Calcium content in the mineralized nodules formed by these cells stimulated with both 300 ng/ml of rhBMP-2 and 25 μM of PD98059 was increased 1.8-fold as compared with that stimulated with 300 ng/ml of rhBMP-2 only (Fig. 2E).

Effects of overexpression of constitutively active or dominant-negative MEK-1 on rhBMP-2–induced osteoblastic differentiation of C2C12 cells

To further confirm the involvement of MAPK signaling on the osteoblastic differentiation, we established two C2C12 cell clones stably expressing constitutively active MEK-1 (CA1 and CA2), two clones expressing dominant-negative mutant (DN1 and DN2), and one mock vector–expressing clone as a control. Immunoblot analysis confirmed the expression of HA-tagged MEK-1 in CA1, CA2, DN1, and DN2 (Fig. 3A, upper panel). When parental C2C12 cells and five transfectants were cultured in DMEM supplemented with 10% FBS for 3 days, the phosphorylation level of MAPK was 56.4% in mock transfectant and >80% in CA transfectants (83.8% in CA1 and 86.1% in CA2) and relatively lower (42.7% in DN1 and 52.5% in DN2) in DN transfectants (Fig. 3A, middle and lower panels).

Morphologically, DN transfectants showed a fibroblast-like shape and their nucleus shape was clear (Fig. 3B, c and d), and two CA transfectants represented a round to spindle-shape with an unclear nucleus under phase-contrast microscopy (Fig. 3B, e and f).

DN transfectants showed higher ALP activity than the mock transfectant, whether they were treated with or without rhBMP-2 (Fig. 3C). In contrast, both CA1 and -2